

A Chemistry-Inspired Framework for Achieving Consensus in Wireless Sensor Networks

Massimo Monti, *Student Member, IEEE*, Luca Sanguinetti, *Member, IEEE*, Christian Tschudin, *Member, IEEE*, and Marco Luise, *Fellow, IEEE*

Abstract—The aim of this paper is to show how simple interaction mechanisms, inspired by chemical systems, can provide the basic tools to design and analyze a mathematical model for achieving consensus in wireless sensor networks, characterized by balanced directed graphs. The convergence and stability of the model are first proven by using new mathematical tools, which are borrowed directly from chemical theory, and then validated by means of simulation results, for different network topologies and number of sensors. The underlying chemical theory is also used to derive simple interaction rules that may account for practical issues, such as the estimation of the number of neighbors and the robustness against perturbations. Finally, the proposed chemical solution is validated under real-world conditions by means of a four-node hardware implementation where the exchange of information among nodes takes place in a distributed manner (with no need for any admission control and synchronism procedure), simply relying on the transmission of a pulse whose rate is proportional to the state of each sensor.

I. INTRODUCTION

The implementation of wireless sensor networks (WSNs) poses several technical challenges. One of primary importance is conjugating the relative unreliability of a single sensor (due to its limited complexity and energy availability) with the high reliability required by certain applications (surveillance, healthcare, factory-automation, in-vehicle sensing and so forth). For this reason, an intense research activity has been devoted to design algorithms whereby clusters of sensors may reach an agreement on certain quantities of interest in a distributed manner, increasing in this way the system reliability. This problem is known in the literature as the *consensus problem* and has received great attention from many different research communities (in computer science, control and information theory, wireless communications and signal processing). A good survey and treatment of the results obtained in this field can be found in [1] – [4] and references therein. Although not only limited to these cases, the existing works are basically inspired by different mechanisms (such as biological interactions [5] – [6], formation control [7], spreading of gossip in social networks [8], synchronization of coupled oscillators [9], belief propagation [10] and so forth), rely on different communication infrastructures (synchronized

[11] or non-synchronized [2] and [8], with or without admission control [12] – [14], clustered-based [15], packet-oriented [8], and so forth) and might make use of different *a-priori* information (e.g., knowledge about the network topology [16]).

In this work, we focus on WSNs characterized by balanced directed graphs (i.e., graphs in which in-degree and out-degree of each node are the same) and propose to look at the consensus problem through the eyes of a chemist. To this end, we first introduce the key concepts of distributed artificial chemistry, which provide basic mathematical tools to (i) formalize interactions among distributed nodes in a chemical manner, (ii) model the dynamics of the resulting chemical reaction networks in the form of ordinary differential equations (ODEs) and (iii) predict the system's equilibrium points. We then use these tools to solve the problem at hand. As we will see, the use of distributed artificial chemistry leads to a consensus model in the same form of that proposed in [1]. Differently from [1], the underlying distributed artificial chemistry lets naturally emerge the interaction mechanisms that are required to drive the dynamical system of each node, in order to operate according to the ODEs. Indeed as we will show, distributed artificial chemistry, besides representing a systematic method to design and analyze distributed systems, represents also a powerful tool to define the microscopic interactions and rules that are needed to achieve macroscopic requirements (thanks to the application of basic chemical rules, such as the law of mass action and the conservation principle). Furthermore, the use of chemical theory allows making use of new analytical tools, such as steady-state and stability analysis, deficiency zero theorem [17] and chemical organization theory [18]. In this work, as a first attempt in this direction, the convergence and stability of the derived mathematical model are proven by using the deficiency zero theorem [19].

The performance of the chemical interaction mechanisms is validated by means of simulation results under different operating conditions and settings (i.e., different network topologies and number of sensor nodes). Comparisons are made with existing solutions based on gossip protocols. Finally, the underlying chemical theory is exploited to include, in the dynamical system, mechanisms to account for some practical issues, such as the estimation of the number of neighboring nodes as well as perturbations.

To validate the proposed solution and to demonstrate that the chemical paradigm is not a mere intellectual exercise, we also present some real measurements obtained from a four-node hardware testbed. In this simple implementation, the

M. Monti and C. Tschudin are with the Department of Mathematics and Computer Science, University of Basel, Bernoullistrasse 16, 4056 Basel, Switzerland (e-mail: {m.monti,christian.tschudin}@unibas.ch).

L. Sanguinetti and M. Luise are with the Dipartimento di Ingegneria dell'Informazione, University of Pisa, Via Caruso 16, 56126 Pisa, Italy (e-mail: {luca.sanguinetti, marco.luise}@iet.unipi.it). L. Sanguinetti is also with the Alcatel-Lucent Chair on Flexible Radio, Supélec, Gif-sur-Yvette, France (e-mail:luca.sanguinetti@supelec.fr)

information exchange among the spatially distributed sensors takes place by means of the transmission of a pulse whose rate is proportional to the state of each node. The experimental results are in line with analytical and simulation results, and show that the proposed solution performs reasonably well even under real-world conditions.

The first attempt to use distributed artificial chemistry for achieving consensus can be found in [20] and [21], in the context of packet-oriented communication networks. Differently from [20] and [21], the main strength of this work lies in the comprehensive treatment of how to make use of chemistry-inspired mechanisms for achieving consensus in WSNs. Specifically, the major contributions of this work are the following:

- We provide a comprehensive treatment of the chemistry-inspired basic tools to design and analyze distributed interaction mechanisms.
- We show how such tools can be used for (i) constructing a consensus model for WSNs characterized by balanced directed graphs, and (ii) proving convergence and stability in the derived system.
- Simulation results, obtained with the network simulator OMNeT 4.1 [22], are used to validate the analysis under different network topologies and number of sensor nodes; comparisons are made with other traditional gossip-inspired mathematical models.
- We make use of the underlying chemical theory to account for some practical issues.
- We validate the performance of the proposed approach by means of a four-node hardware implementation, which relies on an emergent and simple communication protocol where nodes exchange their data in an asynchronous manner with no need for admission control. To the best of our knowledge, this is the first time that a chemistry-inspired algorithm is built in a hardware testbed and validated under real-world conditions.

The use of chemical theory in designing and studying the consensus problem must be seen as an alternative way to look at the problem itself. This approach represents an unexplored field, which may provide new tools for the analysis and implementation of algorithms but still requires further investigations. This work is meant to provide a first comprehensive treatment on this topic that ranges from theory to (early) implementation, and we hope it may serve as an incentive for the research community for further explorations in this context.

The remainder of this paper is organized as follows. The system model and consensus problem are briefly introduced in the next section. The key concepts of distributed artificial chemistry are first described and then applied to a simple chemical network in Section III. The chemistry-inspired consensus model is derived, analyzed, and validated through simulations in Section IV. Its extension to account for some practical issues is discussed in Section V and it is again validated with simulations, as well as compared with other gossip-based algorithms. The hardware implementation is illustrated and the related experimental results are reported in Section VI. Additional insights about the chemical approach

and some open issues are discussed in Section VII. Finally, some conclusions are drawn in Section VIII.

II. PROBLEM STATEMENT

We consider a cluster of M low-mobility sensors¹ connected by wireless links and composed of the following basic components: (i) a continuous-time dynamical system whose state evolves in time according to local measurements and states of nearby sensors, and (ii) a radio transceiver operating in a half-duplex manner that is used to transmit to and receive from nearby sensors.

The interaction topology of the wireless sensor network is modeled as a directed graph (digraph) $\mathcal{G} = (\mathcal{V}, \mathcal{E})$ in which $\mathcal{V} = \{\nu_1, \nu_2, \dots, \nu_{|\mathcal{V}|}\}$ is the set of all sensors with $|\mathcal{V}|$ being equal to M while $\mathcal{E} \subseteq \mathcal{V} \times \mathcal{V}$ is the set of edges, with the convention that $(\nu_i, \nu_j) \in \mathcal{E}$ if and only if there exists an edge from ν_i to ν_j (i.e., the information flows from ν_i to ν_j). The structure of a digraph can be described by the $|\mathcal{V}| \times |\mathcal{V}|$ adjacency matrix \mathbf{A} whose generic entry $[\mathbf{A}]_{i,j}$ is equal to 1 if $(\nu_i, \nu_j) \in \mathcal{E}$ and 0 otherwise. As mentioned in the Introduction, we concentrate on balanced digraphs for which the number of edges entering and leaving a node is the same for all nodes, i.e.,

$$\sum_{j \neq i} [\mathbf{A}]_{i,j} = \sum_{j \neq i} [\mathbf{A}]_{j,i} \quad \forall i \in \mathcal{V}. \quad (1)$$

For notational convenience, we denote by \mathcal{N}_i the neighbor set within the transmitting and receiving range of sensor ν_i , i.e.,

$$\mathcal{N}_i = \{\nu_j \in \mathcal{V} \mid (\nu_i, \nu_j) \in \mathcal{E}\}. \quad (2)$$

Denoting by z_i the discretized measurement of sensor ν_i , the goal of this work is to design, analyze and implement a dynamical system to distributively calculate at each node in the network the average of initial values:

$$z_{\text{avg}} = \frac{1}{M} \sum_{i=1}^M z_i. \quad (3)$$

III. PRINCIPLES FOR A CHEMISTRY-INSPIRED DESIGN OF DISTRIBUTED ALGORITHMS

Consider a vessel in which two molecular species S_1 and S_2 (known as reactants) are present and interact with each other according to the following rule (reaction): consuming a molecule S_1 produces a molecule S_2 and vice-versa. It can easily be proven that the above interaction reaches an equilibrium in which molecules S_1 and S_2 are present in the same quantities. This is achieved for any initial concentration of S_1 and S_2 and without being explicitly programmed.

Although simple, such an example (henceforth, called chemical reversible network) shows how an equilibrium can emerge from simple random interactions whose specific outcomes cannot be easily predicted. This makes the chemical metaphor suited for the consensus problem in WSNs as they

¹We consider WSNs organized in hierarchical levels: the lower level nodes cooperate to achieve local consensus with a reliability greater than the one obtained with a single node; intermediate nodes are responsible for conveying the information gathered by the lower level nodes to the control centers.

are inherently characterized by high randomness and unpredictability. The challenge to import the chemical paradigm into such networks relies on designing algorithms, mimicking chemical reactions, so as to enable the achievement of equilibrium points (in accordance with the requirement specification), in a distributed setup. For this purpose, the key concepts for a chemistry-inspired design and analysis of distributed algorithms are revised in the following section.

A. Distributed artificial chemistry

As defined by Dittrich *et al.* in [23], an artificial chemistry \mathcal{AC} is a “*man-made system that is similar to a chemical system*” in which chemical entities (molecules) interact with each other as specified by abstract models. According to [23], an artificial chemistry \mathcal{AC} is univocally defined by the triplet $\mathcal{AC} = (\mathcal{S}, \mathcal{R}, \mathcal{A})$, where \mathcal{S} is the set of molecular species that may appear in a certain chemistry, \mathcal{R} is the set of reaction rules specifying how the molecules interact, and \mathcal{A} is the reaction algorithm describing how and when the reactions are applied. In particular, a reaction rule $r \in \mathcal{R}$ operates according to a given equation whose general form is as follows:

$$r : \sum_{s \in \mathcal{S}} a_{r,s} s \xrightarrow{k_r} \sum_{s \in \mathcal{S}} b_{r,s} s \quad (4)$$

where k_r is a constant parameter (known as reaction coefficient) that contributes to regulate the average rate at which reaction r occurs (see also later), whereas $a_{r,s}$ is the number of molecules of species s consumed by reaction r (known as stoichiometric reactant coefficient) and $b_{r,s}$ is the number of molecules of species s produced by reaction r (known as the stoichiometric product coefficient). Basically, the above equation states that reaction r replaces $a_{r,s}$ -amount of molecules s to produce $b_{r,s}$ -amount of molecules s with an average rate controlled by k_r .

The dynamics of chemical reactions (when which reaction occurs) are described on average by the well-known law of mass action, which essentially states that the average rate of occurrence of a chemical reaction is proportional to its reactant concentrations [24]. That is, the more molecules are present, the more likely reactions become. Mathematically, this means that a chemical reaction $r \in \mathcal{R}$ occurs at a rate $v_r(t)$ proportional to the abundance of involved reactants:

$$v_r(t) = k_r \prod_{s \in \mathcal{S}} c_s^{a_{r,s}}(t) \quad (5)$$

where $c_s(t)$ denotes the molecular concentration of reactant species s at time t and k_r is the reaction coefficient mentioned before. In artificial chemistry, the law of mass action is respected by properly setting the time instants indicating how and when a generic reaction must be applied. As mentioned before, such a time setting is handled by the reaction algorithm \mathcal{A} . In all subsequent discussions, we rely on a deterministic version of the algorithm introduced by Gibson and Bruck in [25]. For completeness, we report algorithm \mathcal{A} in Appendix A.

The formal definition of an \mathcal{AC} can be extended to a network with digraph $\mathcal{G} = (\mathcal{V}, \mathcal{E})$, by simply introducing the concept

of distributed \mathcal{AC} . Therein, molecules can be exchanged over the network links by executing reaction rules that generate remote actions. In particular, at each node $\nu_i \in \mathcal{V}$, a reaction algorithm \mathcal{A} (the same for all nodes) updates a local multiset of molecules according to a set of local reaction rules. That is, each node ν_i defines a local artificial chemistry as the triplet $\mathcal{AC}_i = (\mathcal{M}_i, \mathcal{R}_i, \mathcal{A})$ in which $\mathcal{M}_i = \mathcal{S}_i \cup \mathcal{S}_i^{(j)}$. The set \mathcal{S}_i defines the species of all molecules that can possibly be found in the local multiset, whereas $\mathcal{S}_i^{(j)} \subseteq \cup_{j \in \mathcal{N}_i} \mathcal{S}_j$ is the set of species that can possibly be found in its neighbors. Each node also defines its own set of reaction rules \mathcal{R}_i where a reaction $r_i \in \mathcal{R}_i$ is specified as follows:

$$r_i : \sum_{s \in \mathcal{S}_i} a_{r_i,s} s \xrightarrow{k_{r_i}} \sum_{s \in \mathcal{M}_i} b_{r_i,s} s \quad (6)$$

from which it is observed that all reactants are local species whereas products may also be species located in the neighboring sensors. This is how transmission or exchange of information is modeled in a chemical way: by allowing a reaction to create products in nearby sensors. Since reactions occur (thanks to the reaction algorithm \mathcal{A}) with an average rate given by the law of mass action in (5), it follows that the exchange of information (interactions among nodes) occurs proportionally to the abundance of local reactants. Observe also that thanks to the mass conservation principle, if the reaction network forms a closed system, then the total number of molecules is conserved by all reactions and remains constant over time.

B. Dynamical analysis of distributed artificial chemistry

The state transition dynamics of a distributed \mathcal{AC} are fully described by the chemical master equation [26]. Unfortunately, this method becomes too complex in the presence of large reaction networks [27]. A possible solution is to resort to the method illustrated in [28] in which the mean time evolution of the chemical reaction system is examined. This amounts to looking at the time evolution of the abundance of species, and can be mathematically formalized using the following set of ODEs:

$$\dot{c}_s(t) = \sum_{r \in \mathcal{R}} b_{r,s} v_r(t) - \sum_{r \in \mathcal{R}} a_{r,s} v_r(t) \quad \forall s \in \mathcal{S} \quad (7)$$

where $v_r(t)$ is the reaction rate given in (5). Denoting by $\mathbf{v}(t)$ the vector collecting all reaction rates, we may rewrite (7) in matrix form as follows $\dot{\mathbf{c}}(t) = \mathbf{U}\mathbf{v}(t)$ where \mathbf{U} is the stoichiometric matrix whose elements are $[\mathbf{U}]_{s,r} = b_{r,s} - a_{r,s}$. That is, modeling the interactions among nodes according to a distributed \mathcal{AC} allows fully characterizing the system dynamics through a fluid model in the form of ODEs.

C. Chemical reversible network

To ease understanding, consider the chemical network whose graphical illustration is given in Fig. 1(a). The network graph is $\mathcal{G} = (\mathcal{V}, \mathcal{E})$ with $\mathcal{V} = (\nu_1, \nu_2)$ and $\mathcal{E} = \{(\nu_1, \nu_2), (\nu_2, \nu_1)\}$. Each node ν_i defines only a molecular species \mathcal{S}_i so that $\mathcal{S}_1 = \{\mathcal{S}_1\}$ and $\mathcal{S}_2 = \{\mathcal{S}_2\}$. This means that $\mathcal{S}_1^{(2)} = \{\mathcal{S}_2\}$ and $\mathcal{S}_2^{(1)} = \{\mathcal{S}_1\}$ whereas $\mathcal{M}_1 = \mathcal{M}_2 =$

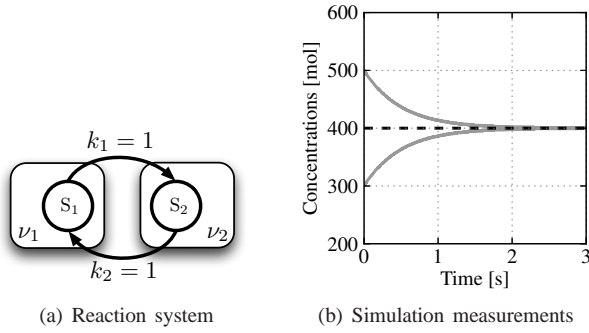


Fig. 1: Chemical reversible network - The chemical reaction system (a) exhibits an equilibrium point wherein concentrations (gray-continuous line in Fig. 1(b)) converge to the arithmetic mean (black-dashed line in Fig. 1(b)) of their initial concentration values (300 and 500).

$\{S_1, S_2\}$. Additionally, each node defines a single reaction rule that consumes one instance of local S-molecules to produce one instance of remote S-molecules. This leads to the following “spatially distributed” reactions: $r_1 : S_1 \rightarrow S_2$ and $r_2 : S_2 \rightarrow S_1$. Collecting all the above facts together yields $\mathcal{AC}_1 = \{\{S_1, S_2\}, r_1, \mathcal{A}\}$ and $\mathcal{AC}_2 = \{\{S_1, S_2\}, r_2, \mathcal{A}\}$. From (7), we thus have that concentrations change over time according to the following set of ODEs:

$$\dot{c}_{S_1}(t) = c_{S_2}(t) - c_{S_1}(t) \quad (8a)$$

$$\dot{c}_{S_2}(t) = c_{S_1}(t) - c_{S_2}(t) \quad (8b)$$

where we have taken into account that the stoichiometric and reaction coefficients of r_1 and r_2 are all equal to one.

When reaching equilibrium at time instant $t = t^*$, the abundances do not change (i.e., $\dot{c}_{S_1}(t^*) = \dot{c}_{S_2}(t^*) = 0$) and the two molecular species are present in the same quantities i.e., $c_{S_1}(t^*) = c_{S_2}(t^*)$. Therefore, by denoting the initial amount of molecules of species i as $c_{S_i}(0)$ and studying (8) at equilibrium, we obtain

$$c_{S_1}(t^*) = c_{S_2}(t^*) = \frac{c_{S_1}(0) + c_{S_2}(0)}{2} \quad (9)$$

that proves that the simple chemical interaction mechanisms defined by \mathcal{AC}_1 and \mathcal{AC}_2 enable to balance the number of molecules between the two nodes. In Fig. 1(b), we report $c_{S_1}(t)$ and $c_{S_2}(t)$ as a function of time t when $c_{S_1}(0) = 500$ and $c_{S_2}(0) = 300$. The results are obtained in the network simulator OMNeT 4.1 by letting two nodes operate according to the artificial chemistries \mathcal{AC}_1 and \mathcal{AC}_2 . As we can observe, the concentrations of the two species converge to the arithmetic mean of the initial values (black-dashed line).

Remark: Although simple, this example is instrumental to understand what mentioned in the Introduction: modeling network interactions as a distributed artificial chemistry \mathcal{AC} provides (i) the microscopic mechanisms (the reactions and their time intervals of execution through reaction algorithm \mathcal{A}) to achieve a specific macroscopic requirement (the average) as well as (ii) ODEs that are needed to describe the network dynamics and to eventually compute its equilibrium points.

IV. A CHEMICAL CONSENSUS MODEL FOR WIRELESS SENSOR NETWORKS

As mentioned in the Introduction, the first attempt to make use of distributed artificial chemistry for achieving consensus can be found in [20], where the authors propose a chemical networking protocol known as *Disperser*. The latter is essentially based on the idea of extending the chemical reversible mechanism illustrated in Section III.C to a network with multiple nodes. In particular, each node ν_i is assumed to contain a molecular species S_i (i.e., $S_i = \{S_i\}$) and to randomly interact with one of its neighboring node ν_j through a spatially distributed reaction $r_{i,j}$. Specifically, reaction $r_{i,j}$ consumes a single S_i -molecule in the local set of node ν_i and remotely produces a single S_j -molecule in one of the neighboring nodes (i.e., $S_i^{(j)} \in \cup_{j \in \mathcal{N}_i} \{S_i\}$). Mathematically, $r_{i,j}$ is formulated as $r_{i,j} : S_i \rightarrow S_j$. As basically done for the chemical reversible network, the above interactions are proven to converge towards the average of the initial measurements by simply relying on the mass conservation principle [20]. From the mathematical expression of remote reactions $r_{i,j}$, it follows that the *Disperser* requires each reaction to be associated with a mono-directional link ($r_{i,j}$ consumes a single S_i -molecule in ν_i and remotely produces a single S_j -molecule in ν_j). This is why the authors in [20] make use of a packet-oriented protocol that basically gives each node the possibility to discern the transmission to and the reception from its neighbors. Although possible, the use of packet-oriented protocols does not match well the less-demanding communication requirements (in terms of routing and address-managing computation) of WSNs composed by sensors of limited complexity and energy availability. Following works such as [2], [3], [13], [14], we show next how to extend the chemical paradigm illustrated above to develop a mathematical model in which the interaction mechanisms take advantage of the broadcast nature of the wireless medium to achieve consensus.

A. Derivation

We start setting $c_{S_i}(0) = z_i$ and defining the following “broadcast” reaction:



from which it follows that the consumption of a single molecule S_i at node ν_i produces one instance of S-molecule at all of its neighbors. This is exactly how broadcast transmission can be modeled in a chemical way. According to the law of mass action in (5), the above reaction occurs at a rate equal to the concentration of the local state, i.e.,

$$v_{i,B}(t) = c_{S_i}(t). \quad (11)$$

Observe now that the execution of $r_{i,B}$ at each node increases the total number of molecules in the network with no limits, thereby violating the mass conservation principle. To overcome this “diffusion phenomenon”, we need to further define a reaction that drains the abundance of S-molecules at each node on the basis of the number of its neighbors. Mathematically,

this amounts to locally performing at each node the following "draining" reaction:



whose rate of occurrence is given by

$$v_{i,D}(t) = (|\mathcal{N}_i| - 1) c_{S_i}(t) \quad (13)$$

as it follows applying (5). Collecting all the above facts together, the artificial chemistry of node ν_i is defined as

$$\mathcal{AC}_i = \{\mathcal{M}_i, \mathcal{R}_i, \mathcal{A}\} \quad (14)$$

with $\mathcal{M}_i = \mathcal{S}_i \cup \mathcal{S}_i^{(j)}$, $\mathcal{S}_i = \{S_i\}$, $\mathcal{S}_i^{(j)} = \{S_j | j \in \mathcal{N}_i\}$ and $\mathcal{R}_i = \{r_{i,B}, r_{i,D}\}$.

Then, from (7) using (10) and (12) we have that the ODEs describing the evolution of c_{S_i} take the form:

$$\dot{c}_{S_i}(t) = \sum_{j \in \mathcal{N}_i} c_{S_j}(t) - |\mathcal{N}_i| c_{S_i}(t), \quad c_{S_i}(0) = z_i. \quad (15)$$

Recalling that $[\mathbf{A}]_{i,j} = 1$ for any $j \in \mathcal{N}_i$ and observing that

$$|\mathcal{N}_i| = \sum_{j \in \mathcal{N}_i} [\mathbf{A}]_{i,j} \quad (16)$$

we may rewrite (15) as

$$\dot{c}_{S_i}(t) = \sum_{j \in \mathcal{N}_i} [\mathbf{A}]_{i,j} (c_{S_j}(t) - c_{S_i}(t)) \quad (17)$$

or, equivalently, in matrix form

$$\dot{\mathbf{c}}_S(t) = -\mathbf{L}\mathbf{c}_S(t) \quad (18)$$

where \mathbf{L} is Laplacian matrix of \mathcal{G} and \mathbf{c}_S is the vector collecting all species concentrations (nodes' state). The latter is exactly in the same form of the mathematical model proposed in [29] and is known to converge towards the average of the initial measurements as formulated in (3) when \mathcal{G} is a strongly connected and balanced digraph. Therefore, mimicking sensor interactions in WSNs through distributed artificial chemistries has given us the tools to derive a mathematical model whose convergence to the average is guaranteed in the investigated scenario. In contrast to [29], the underlying chemical theory allows making use of analytical tools never used in this context before. Indeed, in Appendix B we show how the deficiency zero theorem can be used to prove the convergence and stability of (15). To our knowledge, this is the first time that such a tool is used for proving the convergence of consensus algorithms.

B. Simulation results

In this subsection, the performance of the consensus model in (18) is validated under different operating conditions (different network topologies and number M of sensors²) by means of simulation results obtained with the network simulator OMNeT 4.1. Observe that, thanks to the underlying chemical framework, the simulation of (18) requires only to let the

²Due to space limitations, we cannot provide a complete numerical analysis of all the investigated settings. However, all available results will be provided upon request.

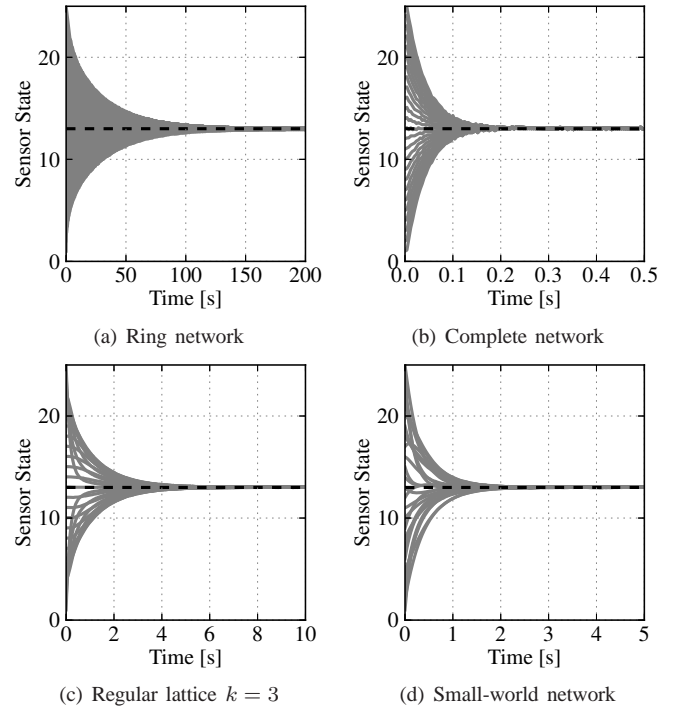


Fig. 2: Sensors' state evolution obtained when $M = 25$ sensors are connected through (a) a ring network, (b) a complete network, (c) a regular lattice network topology with interconnections to $k = 3$ nearest neighbors, and (d) a small-world network topology with $3M$ links (see [1] and references therein for more details on such networks). The initial state is set to $z_i = i$ for $i = 1, 2, \dots, M$.

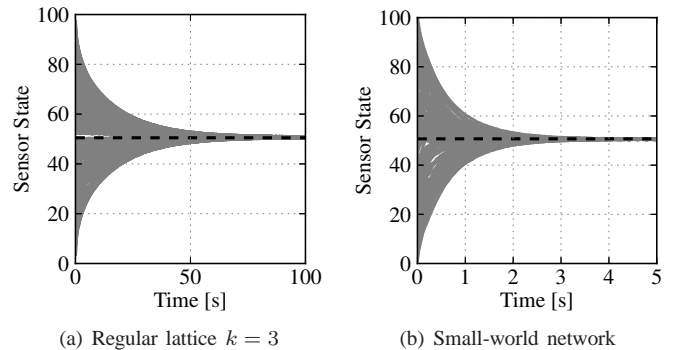


Fig. 3: Sensors' state evolution obtained when $M = 100$ sensors are connected through (a) a regular lattice network topology with interconnections to $k = 3$ nearest neighbors and (b) a small-world network topology with $3M$ links. The initial state is set to $z_i = i$ for $i = 1, 2, \dots, M$.

dynamical system of each node ν_i operate according to the artificial chemistry defined in (14). It is worth observing that no synchronous models and admission control mechanisms are required by \mathcal{AC}_i . Sensor interactions take place through reactions that are applied according to the time instants of the reaction algorithm \mathcal{A} , driven by the law of mass action. This makes the implementation of the dynamical system a simple task.

TABLE I: Convergence times for achieving a normalized mean squared error less than 0.01 with different network topologies.

	$M = 25$	$M = 50$	$M = 100$	$M = 250$	$M = 1000$
Ring network	80 s	230 s	450 s	900 s	1250 s
Regular lattice with $k = 3$	4 s	12 s	35 s	90 s	180 s
Small-world network with $3M$ links	1 s	1 s	1 s	1 s	1 s
Complete network	0.26 s	0.09 s	0.04 s	0.012 s	0.005 s

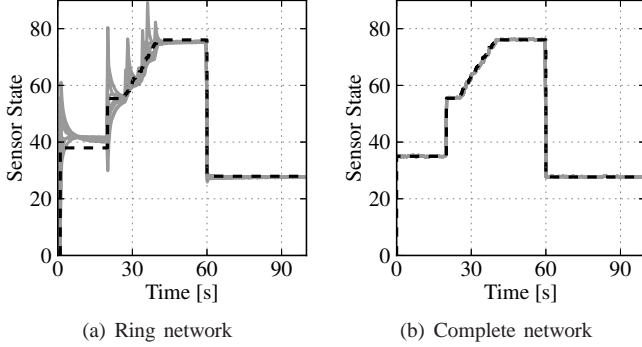


Fig. 4: Sensors' state evolution when $M = 30$ sensors are connected through (a) a ring and (b) a complete network topology. Sensors' measurements vary as follows: at time $t = 0, 20,$ and 60 (in s) the sensor measurements are independent random variables chosen uniformly within the intervals $[5, 30]$, $[50, 60]$ and $[25, 35]$, respectively. During the time interval between $[25, 40]$, each sensor independently chooses a time instant to change its measurement, chosen uniformly within the interval $[75, 77]$.

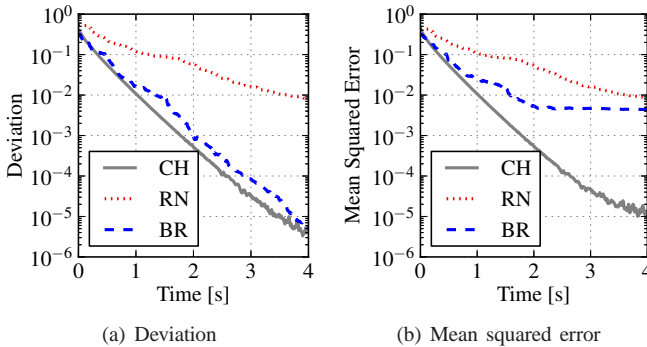


Fig. 5: Performance comparisons among the chemical (CH) consensus algorithm, the broadcast (BR) and randomized (RN) gossip algorithms. Initial state and network setup are as in Fig 3(b).

Fig. 2 demonstrates the convergence of the sensor's state towards the arithmetic mean for different network topologies (ring, complete, regular lattice, and small world networks), when the number of nodes is $M = 25$. These results are in line with those in [1]: compared to the other networks, small-world networks exhibit shorter convergence times, while still keeping the number of links reasonably low. This occurs thanks to the

algebraic connectivity of the associated digraph \mathcal{G} .³ To ease the comparison of the chemical algorithm's dynamics with those of the traditional model in [1], we also report in Fig. 3 the convergence time when $M = 100$ sensors are connected through a regular lattice and a small-world network (refer to Fig. 4 in [1]).

Table I reports the convergence times required by the artificial chemistry to reach a normalized mean squared error equal to 0.01 for different numbers of nodes and different network topologies. The initial state is set as $z_1 = 60$ and $z_i = 30$ with $i = 2, 3, \dots, M$. From the results of Table I, we can see that the convergence time of a complete network decreases substantially as M becomes larger due to the exponential increase of the number of connected links. The opposite happens for a ring network as, in this case, the information is exchanged in a serial manner and thus, the time required to exchange information among all nodes highly grows with increasing number of nodes. On the other hand, the convergence time remains constant for small-world networks.

Fig. 4 illustrates sensors' state evolution when the network is composed of $M = 30$ nodes and is characterized either by a ring or a complete topology. To validate the convergence of the algorithm in presence of measurement changes, the quantities z_i are randomly generated (at certain time instants) according to a uniform distribution with given intervals (see Fig. 5 for details). From the experimental results in Fig. 4, it follows that the convergence to each new value of the arithmetic mean is guaranteed for both network topologies. This holds true only if the measured quantities vary sufficiently slow compared to the convergence time. As we can observe, due to the different algebraic connectivity, the convergence is achieved almost instantaneously for the complete network, whereas a longer time interval is required for the ring network.

Comparisons are also made with the two following consensus gossip-based algorithms: the randomized (RN) solution proposed in [8] and the broadcast (BR) one illustrated in [2]. Both algorithms are simulated according to the asynchronous model described in [8] and [2], whereby each node is assumed to have a clock that ticks independently according to a rate μ Poisson process. This corresponds to a single global clock whose ticking times form a Poisson process of rate $M\mu$ [2]. In all subsequent simulations, we set an average of $\mu = 2$ ticks per second in each node. When RN is used, at each tick, node ν_i randomly interacts with a single nearby sensor. On the other hand, node ν_i wirelessly broadcasts its current state value when BR is applied. Comparisons are made in

³The algebraic connectivity is the second smallest eigenvalue λ_2 of the associated digraph \mathcal{G} . The higher λ_2 is, the lower the convergence time is. Related to results in Fig. 2, λ_2 is found to be 0.0314, 25, 0.8523, and 2.0269 for the ring, complete, regular lattice, and small-word networks, respectively.

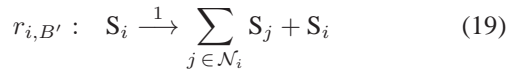
terms of the normalized deviation of sensors' states from their average and of the mean squared error w.r.t. the average of their initial states (measured quantities z_i). For this purpose, we consider the same operating conditions as in Fig. 3(b): a small world network with $M = 100$ nodes and $3M = 300$ links in which the initial states are set to $z_i(0) = i$ for $i = 1, 2, \dots, M$. The results of Fig. 5(a) show that the convergence time of the proposed chemical (CH) algorithm is similar to that experienced with the BR algorithm. As seen, both largely outperform RN, which does not take advantage of the broadcast nature of the wireless medium. On the other hand, Fig. 5(b) shows that the estimation accuracy of the CH algorithm is higher than that of the BR algorithm. This difference is due to the bias term that the BR algorithm introduces in the average estimation. For further details, the interested reader is referred to [30], in which a solution to overcome this problem is also discussed. However, this is achieved at the price of a higher convergence time and a more complex communication model that requires the transmission and the processing of a "companion" variable, in addition to the node's state. In summary, the results of Fig. 5 show that the proposed CH algorithm allows one to achieve a good trade-off between convergence time and estimation accuracy.

V. SOME PRACTICAL ISSUES

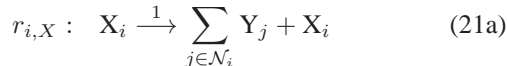
In this section, we discuss how to modify the chemistry-inspired dynamical system of each sensor to account for some practical issues.

A. Estimating the number of neighbors

Observe that the execution of $r_{i,D}$ in (12) requires knowledge of $|\mathcal{N}_i|$, which is hardly available at each node, especially in those applications in which nodes appear and disappear over time. To address this issue, we start rewriting (10) and (12) as follows:



The above operation has no effect on the dynamics of \mathcal{A}_i (same set of ODEs as in (15)) and it is only used to make the system depend on $|\mathcal{N}_i|$ rather than $|\mathcal{N}_i| - 1$.⁴ To proceed further, we let each node ν_i define two molecular species X_i and Y_i , with X_i characterized by a constant concentration equal to λ , i.e., $c_{X_i}(t) \equiv \lambda$. Then, we define the following reactions:



Using (7) and recalling that $c_{X_i}(t) = \lambda$ yields

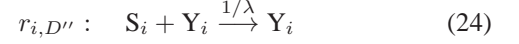
$$\dot{c}_{Y_i}(t) = \lambda |\mathcal{N}_i| - c_{Y_i}(t) \quad (22)$$

⁴This allows overcoming some implementation issues. First, computing the difference $|\mathcal{N}_i| - 1$ would require an additional set of reactions (see for example the motif proposed in Section 10.3 of [20]). Second, using (19) and (20) allows maintaining the sensor state also in a single-node network.

from which it follows that at the equilibrium (i.e., $\dot{c}_{Y_i}(t^*) = 0$) the abundance of Y-molecules at each node is $\lambda |\mathcal{N}_i|$:

$$c_{Y_i}(t^*) = \lambda |\mathcal{N}_i|. \quad (23)$$

Then, replacing the draining reaction $r_{i,D'}$ with



yields the following ODEs

$$\dot{c}_{S_i}(t) = \sum_{j \in \mathcal{N}_i} c_{S_j}(t) - \frac{1}{\lambda} c_{Y_i}(t) c_{S_i}(t), \quad c_{S_i}(0) = z_i. \quad (25)$$

from which, by assuming that the convergence time of (21a) and (21b) is smaller than that required by (19) and (24) and thus by substituting (23) in (25), we get the following result

$$\dot{c}_{S_i}(t) = \sum_{j \in \mathcal{N}_i} c_{S_j}(t) - |\mathcal{N}_i| c_{S_i}(t), \quad c_{S_i}(0) = z_i. \quad (26)$$

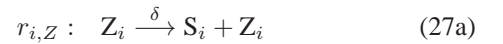
Equation (26) is in the same form as (15) but has been obtained without knowing $|\mathcal{N}_i|$, simply by using the reactions in (21) and modifying the draining reaction as in (24).

Remark: Observe that the above results hold true only if (21a) and (21b) reach the equilibrium before (19) and (24). This is reasonable for low-mobility applications but can generally be achieved by properly setting the design parameter λ , which dictates the rate of execution of (21a). The higher the λ -coefficient is, the faster the convergence is.

Remark: In those applications where $|\mathcal{N}_i|$ remains constant for a long time interval, its value can be easily estimated through artificial chemistry \mathcal{A}_i defined in (14) (with no need for additional reactions): During an initialization phase, the sensors' state should be maintained constant at the pre-defined value λ (i.e., $c_{S_i}(t) = \lambda$) and the reaction $r_{i,D}$ should not be locally executed. In these cases, the execution of $r_{i,B}$ would induce the production of S-molecules in nearby sensors with an average rate $|\mathcal{N}_i|$ times bigger than the pre-defined value λ (this easily follows recalling the broadcast nature of reaction $r_{i,B}$). Therefore, an estimate of $|\mathcal{N}_i|$ could be easily obtained by comparing the measured reception rate and the predefined one.

B. Robustness to perturbations

A WSN must be robust to possible perturbations, such as measurement errors or sensors leaving (entering) the network in advance (at a later stage). To chemically address these issues, we let each node define a molecular species Z_i whose concentration is maintained constant and equal to the local measurement value, i.e., $c_{Z_i}(t) = z_i$. Then, we introduce the two following reactions:



with δ being a design parameter. The execution of $r_{i,Z}$ continuously feeds S_i -species at a rate δ -proportional to the local measurement z_i . At the same time, S_i -species is drained with the same coefficient δ of proportionality through reaction $r_{i,A}$. As a result, sensors' state (the concentration of molecules

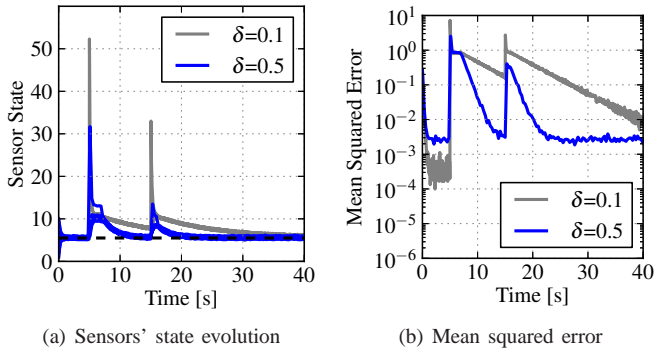


Fig. 6: Effect of δ on the recovery from perturbations in a small world network with $M = 10$ nodes, $3M = 30$ links. The initial state is $z_i = i$ for $i = 1, 2, \dots, M$. At $t = 5$, node ν_1 introduces an error of 50% for 2 seconds. At $t = 15$, node ν_4 introduces an error of 30% for 1 second.

S_i) is continuously refreshed and if an error occurs, after a transient time, sensor's state goes back to the correct value. The higher the δ -coefficient is, the faster the recovering is. As shown next by means of simulation results, this is however achieved at the price of a reduced estimation accuracy.

Observe that the dynamics of (28) are described by the following ODE:⁵

$$\dot{c}_{S_i}(t) = \sum_{j \in \mathcal{N}_i} c_{S_j}(t) - |\mathcal{N}_i| c_{S_i}(t) + \delta (z_i - c_{S_i}(t)) \quad (28)$$

whose matrix form is given by

$$\dot{\mathbf{c}}_S(t) = -\mathbf{L}\mathbf{c}_S(t) + \delta(\mathbf{z} - \mathbf{c}_S(t)) \quad (29)$$

where \mathbf{L} is the graph Laplacian of the network. Rewriting (29) after taking the Laplace transform of both sides at a certain reference time $t = t'$, we get

$$\mathbf{C}_S(s) = \mathbf{H}(s)(\mathbf{c}_S(t') + \delta\mathbf{z}) \quad (30)$$

where $\mathbf{H}(s)$ is the Laplacian transfer function given by

$$\mathbf{H}(s) = (s\mathbf{I}_M + \mathbf{L} + \delta\mathbf{I}_M)^{-1} \quad (31)$$

with \mathbf{I}_M being the identity matrix of order M . One can use $\mathbf{H}(s)$ to analytically evaluate how the δ -coefficient must be chosen: a trade-off between the convergence time and estimation accuracy.

C. Simulation results

To account for the above mechanisms, the dynamical system of each node must simply be modified so as to operate according to the new artificial chemistry given by

$$\mathcal{AC}'_i = \{\mathcal{M}'_i, \mathcal{R}'_i, \mathcal{A}\} \quad (32)$$

with $\mathcal{M}'_i = \mathcal{S}'_i \cup \mathcal{S}_i^{(j)'}$, $\mathcal{S}'_i = \{\mathcal{S}_i, \mathcal{X}_i, \mathcal{Y}_i, \mathcal{Z}_i\}$, $\mathcal{S}_i^{(j)'} = \{\mathcal{S}_j, \mathcal{Y}_j | j \in \mathcal{N}_i\}$ and

$$\mathcal{R}'_i = \{r_{i,B'}, r_{i,D''}, r_{i,X}, r_{i,Y}, r_{i,Z}, r_{i,A}\}. \quad (33)$$

⁵ \mathbf{z} represents the vector of initial states.

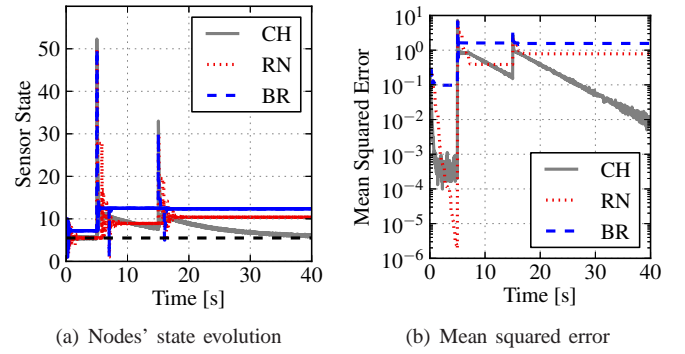


Fig. 7: Performance comparisons among the chemical consensus (CH) algorithm and the broadcast (BR) and randomized (RN) gossip algorithms in presence of perturbations. At $t = 5$, node ν_1 introduces an error of 50% for 2 seconds. At $t = 15$, node ν_4 introduces an error of 30% for 1 second. Coefficient δ is set to 0.1, and initial state and network setup are as described in Fig. 6.

We begin by assessing the impact of δ . As mentioned before, the dimensioning of δ represents a trade-off between robustness to perturbations and estimation accuracy. In Fig. 6, we illustrate sensors' state evolution and mean squared error of CH algorithm when δ is either 0.1 or 0.5. In this experiment, certain nodes exhibit transient problems in sensing or transmitting, and thus introduce some perturbations in the chemical network. The results of Fig. 6 show that a higher value of δ allows a faster recovery from perturbations at the expense of a lower estimation accuracy. As shown in Fig. 6(b), the mean squared error during the first five seconds is less than 10^{-3} for $\delta = 0.1$ whereas it is higher than 10^{-3} for $\delta = 0.5$. Simulation results (not shown for space limitations) show that $\delta = 0.1$ allows achieving a good tradeoff between the two conflicting requirements. For this reason, we set $\delta = 0.1$ in all subsequent simulations.⁶

Fig. 7 illustrates performance comparisons among CH, BR, and RN algorithms, in the same perturbed scenario as in Fig. 6. The CH algorithm results to be resilient to measurement errors (perturbations) while RN and BR do not guarantee the achievement of average consensus. A simple (but inefficient) solution to make RN and BR recover from errors would be that of including a mechanism that automatically switches off all sensors and lets them run with the new measurements. However, this should be done whenever a perturbation occurs.

Fig. 8 illustrates the performance of CH, RN, and BR in the operating conditions described in Fig. 6. This time, node ν_1 suddenly disappears at time $t = 5$ whereas node ν_{10} only appears at $t = 20$. As we can see, the correction mechanism introduced in CH lets nodes track the variations induced in the average value by the intermitting communications, while RN and BR fail.

⁶Different values of parameter δ may be required in scenarios exhibiting different features (e.g., affected by perturbations of different intensity) or for different application constraints (e.g., a different estimation accuracy constraint).

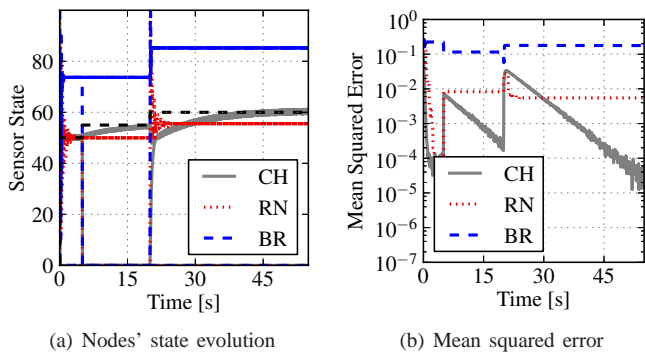


Fig. 8: Performance comparisons among the chemical consensus (CH) algorithm and the broadcast (BR) and randomized (RN) gossip algorithms in presence of perturbations. The initial state is $z_i = 10i$ for $i = 1, 2, \dots, M$. At $t = 5$, node ν_1 disappears whereas node ν_{10} switches on at $t = 20$. Coefficient δ is set to 0.1 and the network setup is as described in Fig. 6.



Fig. 9: Experiment testbed consisting of four sensors where the dynamical system is implemented in the embedded processor TI-MSP430F5438A, and the radio transceiver through transmitter TXM-433-LR, receiver RXM-433-LR, and comparator MAX-921. Sensors are implemented on TI-CC1120 evaluation board which has also an LCD display for a practical setup and tracking of run-time computation.

VI. HARDWARE IMPLEMENTATION AND EXPERIMENTAL RESULTS

In this section, we report on the experimental results obtained with a four-node hardware implementation (see Fig. 9), operating according to the artificial chemistries defined in (32) and (33). To our knowledge, this is the first time that a chemistry-inspired algorithm is built in a hardware testbed and validated under real-world conditions, where nodes exchange their data in an asynchronous manner with no need for admission control.

A. Hardware implementation

The dynamical system, operating according to artificial chemistry specifications, is implemented into an embedded processor TI-MSP430F5438A, which is also used for data acquirement and conversion. The radio interface (transceiver)

is developed with a simple low-cost circuit using the TXM-433-LR integrated chip for transmitting to and the RXM-433-LR integrated chip for receiving from nearby nodes. To limit the complexity of each node, we let the sensor interactions occur in a simple manner. Specifically, we assume that a pulse $g_\tau(t)$ of duration τ is sent over the channel whenever the remote reaction $r_{i,B'}$ in (33) is executed (in the dynamical system). On the other hand, the production of an S-molecule is induced whenever a pulse $g_\tau(t)$ is received from nearby sensors. According to the law of mass action in (5), the average rate of occurrence of $r_{i,B'}$ is proportional to the concentration of S-molecules (sensor's state). This means that the spatially distributed nodes interact by means of pulses whose transmission rate encodes nodes' state. Following the same line of reasoning, we let a pulse $g_{\tilde{\tau}}(t)$ of duration $\tilde{\tau} \neq \tau$ be sent whenever the remote reaction $r_{i,X}$ is executed, and a Y-molecule be produced whenever $g_{\tilde{\tau}}(t)$ is received.

Remark To ease understanding, consider a simple network only composed by $M = 2$ nodes. Without loss of generality, we concentrate on the first node and explain how sensor interactions occur. The node starts transmitting pulses $g_\tau(t)$ at a rate equal to the initial concentration of its local species (value equal to the measured quantity, i.e., $c_{S_1}(0) = z_1$). At the same time, $c_{S_1}(t)$ is continuously modified on the basis of the number of $g_\tau(t)$ -pulses that are received from node 2. This happens at a rate equal to $c_{S_2}(t)$. Internally, the current state $c_{S_1}(t)$ is also continuously decreased at a rate $c_{S_1}(t)$, according to reaction $r_{1,D'}$ in (20), and modified proportionally to the δ -parameter, according to the reactions reported in (27). To continuously estimate the number of neighbors, node 1 has also to transmit $g_{\tilde{\tau}}(t)$ -pulses at a constant rate λ and to increase $c_{Y_1}(t)$ whenever a pulse $g_{\tilde{\tau}}(t)$ is received from node 2.

Remark: Observe that the pulse rate depends on the sensor's state. However, this does not mean that if $z_i = 10^9$ then 10^9 pulses $g_\tau(t)$ must be transmitted by node ν_i . Indeed, it is important to decide how the values are encoded or, in other words, how a molecule quantity has to be interpreted. Assume for example that the algorithm has to measure the average temperature in a sensor network. Then, in order to limit the pulse rate, one has to properly associate the right quantity to a single molecule instance (degrees celsius, Kelvin, Fahrenheit). This allows controlling the maximum transmission rate at the price of a reduced accuracy of the computation (accuracy in the estimation).

Remark: A possible drawback of the above implementation is that no countermeasures are taken against interferences that might arise in WSNs, when the signals transmitted by multiple nodes collide at a given receiving node. Although a judicious design of the system parameters (maximum value of concentrations, duration of the pulse and so forth) could reduce the occurrence of collisions, more advanced multiple access protocols are required to effectively counteract the above issue, thus increasing the complexity of each sensor. For this reason, we have decided not to take countermeasures against interferences. This choice has also been motivated by the observation that chemical systems usually exhibit strong robustness to perturbations thanks to the mass-action kinetics

TABLE II: Local data z_i detected by node ν_i at time t during the experiment whose results are plotted in Fig.10.

Time instant t [seconds]	0	9.8	19.9	53 \rightarrow 57	63
Value of z_1	50	50	50	50	50
Value of z_2	0	50	50	\rightarrow 0	/
Value of z_3	0	0	20	20	0
Value of z_4	0	0	0	0	0

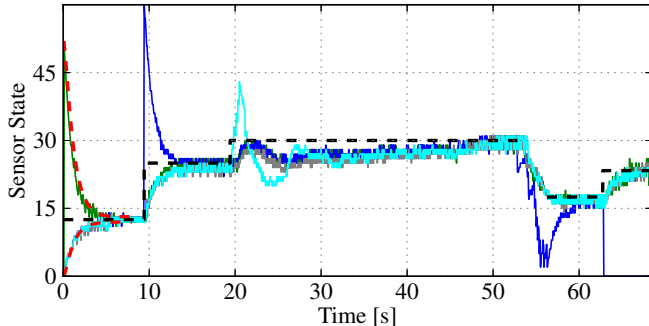


Fig. 10: Experiment results (4 colored, continuous lines) and analytical predictions obtained from (31) (2 red, dashed lines – within the time interval going from $t = 0$ s to $t = 9$), and arithmetic mean (1 black, dashed line). The δ coefficient is set to 0.1.

governing their interaction mechanisms (the interested reader is referred to [31] for a recent work in the context of sensitivity and robustness of chemical reaction systems). Therefore, a chemistry-inspired algorithm is likely to be robust against the unreliable conditions of WSNs.⁷ This has indeed been confirmed in our experiments although only four-node WSNs were tested.

B. Experimental results

The transmitter output power is 3 dBm on average whereas the receiver sensitivity is -120 dBm with a dynamic range of 80 dB. Each sensor is roughly characterized by a total power consumption of 36 mW approximately distributed as follows: 13 mW consumed by the embedded processor, 17 mW by the receiver, and 6 mW by the transmitter. The nodes are placed approximately 7 meters apart from each others, in an indoor environment. The transmission takes place over the free Industrial Scientific Medical radio band $433.05 \div 434.79$ MHz around the carrier frequency of 433.92 MHz. We set $\tau = 200 \mu\text{s}$ and $\tilde{\tau} = 100 \mu\text{s}$, and directly control the quantities z_i (sensor measurements) during the experiment, as shown in Table II. In order to test the robustness of the network against external interferences, we also intentionally let a radio signal interfere with the information exchange within the time interval [22, 33].

Fig. 10 illustrates sensors' state evolution (taken at a sampling rate of 10 ms) of each node ν_i under the above operating

⁷The robustness is a direct consequence of the fact that the information exchange is encoded into a rate rather than in one or few information packets, and thus any corruption of one or few of these transmissions does not affect significantly the system. Another reason for the inherent robustness is that mass action kinetics often induces low-pass filtering behaviors and transfer functions exhibiting negative real-part poles.

conditions. The green, blue, cyan and grey continuous-lines refer to sensors' state evolution of node ν_1 , ν_2 , ν_3 and ν_4 , respectively. The black dashed-line represents the arithmetic mean as obtained through (3) while the red dashed-lines represent the analytical responses of sensor local states as obtained using the Laplacian transfer function in (31). For illustration purposes, only the first 9 seconds of the analytical responses are shown. As we can see, the experimental results are in line with the analytical ones and show that the nodes are able to correctly converge to the desired value after a "short" transient time, regardless of measurement variations and interferences. In particular, it turns out that the effect of the interfering signal (from $t = 22$ to $t = 33$) is that of temporarily making the sensors underestimate the average. Once removed, each sensor converges to the desired value in approximately 20 seconds.

VII. DISCUSSIONS AND OPEN ISSUES

This paper is basically divided into two parts:

1) *Artificial chemistry for consensus in WSNs*: We first show analytically and by means of simulations that simple interaction mechanisms inspired by chemical systems can provide the basic tools for achieving consensus in WSNs. However, some issues are still open.

In this work, we do not cover in details the discretization aspect (studied for example in [32] and summarized in [4]), which may affect the final nodes' average-estimate. We limit to observe here that by calibrating the amount of produced molecules per sensed-quantity unit, designers can regulate the precision of the nodes' estimates and decide the amount of transmissions.⁸ Please observe further that another way to reduce the computations/transmissions, and thus the resource consumption, consists in slowing down the virtual time characterizing the chemical model: transmissions decrease in number, this time, at the cost of a proportionally-slower adaptation (in our simple implementation, lower rates mean lower probability of collisions/interferences).

In this work, we have considered a very simple communication model and referred not to specific channel models and communication technologies. However, we have tested by means of simulations the ability of a chemistry-based system to recover from perturbations. In fact, such perturbations may represent the generalized effect of fading (transient undervalued state of one or more sensors), multipath (transient overvalued state of one or more sensors), or non-reliable links (variation of the number of nodes and different participation times).

This work has focused on balanced digraphs only. In the presence of unbalanced graphs, the theoretical and experimental results illustrated in this paper are no longer valid. Indeed in this case, sensors *converge* to a common value that differs from the average of the local measurements.⁹ This result

⁸In the simulations, we have coped anyway with the effect of discretization: we have had to use a number of molecules per unit quantity so as to obtain acceptable estimation accuracy.

⁹For unbalanced graphs, this work does not represent a solution to constrained consensus problems but it is still a solution to unconstrained consensus problems, according to definitions in [1].

occurs because, at the equilibrium, molecules are still evenly distributed among all participating sensors but are “diffused” with different proportions, depending on the ratios between the number of receiving neighbors and that of transmitting ones. We are currently working on the development of solutions able to take into account such different weights while still using chemical mechanisms of similar complexity to those adopted in this paper.

2) *A simple implementation of artificial chemistry in WSNs:* The second part of the paper shows that the artificial chemistry can work under real-world conditions, and that the above framework can be used directly to develop a hardware implementation. To our knowledge, this is the first time we go beyond the theoretical treatment of chemical algorithms, and prove the applicability (at the lowest networking layers) of the chemical approach in a real sensor network. Although the experimental results are quite promising even under real-world conditions, this work should not be seen as a finalized, ready-to-use commercial product for nowadays markets. We believe that further research in the implementation context may bring significant improvements in terms of robustness and speed.

VIII. CONCLUSIONS

In this paper, we have made use of distributed artificial chemistry to derive and analyze a set of interaction rules that allows achieving consensus in WSNs in a distributed manner, with no need for any synchronism and admission control mechanism. The proposed solution has been first validated and compared with other solutions, by means of experimental results, and then tested under real-world conditions using a four-node hardware implementation. The numerical and experimental results show that the use of artificial chemistry for deriving, analyzing, and implementing communication protocols is not merely an intellectual exercise but an alternative approach, which may pave the way for the development of robust solutions, able to cope with the uncertainties of WSNs.

APPENDIX A: REACTION ALGORITHM

The reaction algorithm \mathcal{A} is reported below.

- 1) Initialize:
 - a) set the initial amount of molecules;
 - b) calculate the value v_r according to (5) $\forall r \in \mathcal{R}$;
 - c) set a putative reaction-execution time $t_r = 1/v_r$ $\forall r \in \mathcal{R}$;
 - d) store t_r values in an indexed priority queue (first stored element has the next reaction time).
- 2) Let r_μ be the reaction whose putative reaction time, t_μ , is least.
- 3) Wait as long as $t < t_\mu$.
- 4) Change the number of molecules to reflect execution of reaction r_μ .
- 5) Update all those reactions, r_α , that depend on the executed reaction r_μ :
 - a) temporarily store the old value $v_\alpha^{old} = v_\alpha$;
 - b) calculate the new value v_α , according to (5);
 - c) if $r_\alpha \neq r_\mu$, scale the reaction execution time as $t_\alpha = (v_\alpha^{old}/v_\alpha)(t_\alpha - t) + t$;

else if $r_\alpha = r_\mu$, set the reaction execution time $t_\alpha = 1/v_\alpha + t$;

- d) store the calculated reaction execution time t_α in the indexed priority queue.
- 6) Go to Step 2.

- * The variable t reflects the current time.
- ** Molecular species represent mere counters. Step 4 implies to decrement all those counters related to the reagent-species (species appearing in (4) on the left-hand side of the arrow) and to increment all those counters related to the product-species (species appearing in (4) on the right-hand side of the arrow).
- *** We consider deterministic inter-reaction times.

APPENDIX B: CONVERGENCE AND STABILITY

We start observing that the dynamics of the reaction network emerging from (10) and (12) at each sensor node $\nu_i \in \mathcal{V}$ are equivalent to those obtained by deploying the following set of reactions at each node ν_i :



To proceed further, we need to briefly introduce the terms “complexes” and “weakly reversible”. Complexes are those multisets of species that appear on the left- and the right-hand side of a reaction, [33]. A chemical reaction network is weakly reversible if for every reaction leading from complex C_i to complex C_j , there is also a chain of reactions leading from C_j back to C_i . According to this definition, the reaction network arising from (34) is weakly reversible. To see how this comes about, observe that all the species of the reaction network are complexes. Moreover, they do correspond also to the graph vertices of the communication network. This means that in strongly connected graphs for every reaction leading from complex C_i to complex C_j there exists a chain of reactions leading from C_j to C_i . In addition, the emergent reaction network is closed (the amount of molecules within the system remains constant).

We now introduce the “deficiency” defined as

$$\gamma = |\mathcal{C}| - l - \text{rank}(\mathbf{U}) \quad (35)$$

where \mathcal{C} denotes the set of complexes, l is the number of linkage classes (i.e., the number of connected subgraphs in the graph of complexes), and $\text{rank}(\mathbf{U})$ denotes the rank of the stoichiometric matrix \mathbf{U} . From (34), it follows that $|\mathcal{C}| = |\mathcal{V}|$ and it can easily be proven that $l = 1$ since each complex is connected directly or indirectly to any other complex constituting the whole digraph. Moreover, a strongly connected chemical reaction network, where every chemical species appears in precisely one complex, has a stoichiometric matrix with rank equal to $\text{rank}(\mathbf{U}) = |\mathcal{V}| - 1$ [34]. Collecting all the above facts together, we have that the deficiency of the reaction network associated to (34) is zero.

According to the Deficiency Zero Theorem [17], if the reaction network is weakly reversible and has a null deficiency value then it has a single, asymptotically-stable fixed point. Setting $\dot{c}_{S_i}(t) = 0$ and studying the equilibrium solution, it follows that the fixed point is defined by the right-hand

side of (3). This proves that the proposed chemical algorithm converges to the average of initial measurements.

REFERENCES

- [1] R. Olfati-Saber, J. Fax, and R. Murray, "Consensus and cooperation in networked multi-agent systems," *Proceedings of the IEEE*, vol. 95, no. 1, pp. 215–233, Jan 2007.
- [2] T. C. Aysal, M. E. Yildiz, A. D. Sarwate, and A. Scaglione, "Broadcast gossip algorithms for consensus," *IEEE Transactions on Signal Processing*, vol. 57, no. 7, pp. 2748–2761, Jul 2009.
- [3] M. Franceschelli, A. Giua, and C. Seatzu, "Distributed averaging in sensor networks based on broadcast gossip algorithms," *IEEE Sensors J.*, vol. 11, no. 3, pp. 808–817, Mar 2011.
- [4] A. G. Dimakis, S. Kar, J. M. F. Moura, M. G. Rabbat, and A. Scaglione, "Gossip algorithms for distributed signal processing," *Proceedings of the IEEE*, vol. 98, no. 11, pp. 1847–1864, Nov 2010.
- [5] S. Barbarossa and G. Scutari, "Bio-inspired sensor network design," *IEEE Signal Processing Magazine*, vol. 24, no. 3, pp. 26–35, May 2007.
- [6] C. Charalambous and S. Cui, "A biologically inspired networking model for wireless sensor networks," *IEEE Network*, vol. 24, no. 3, pp. 6–13, Jun 2010.
- [7] Z. Wu, Z. Guan, Z. Wu, and T. Li, "Consensus based formation control and trajectory tracing of multi-agent robot systems," *J. of Intelligent and Robotic Systems*, vol. 48, no. 3, pp. 397–410, Mar 2007.
- [8] S. P. Boyd, A. Ghosh, B. Prabhakar, and D. Shah, "Randomized gossip algorithms," *IEEE Transactions on Information Theory*, vol. 52, no. 6, pp. 2508–2530, Jun 2006.
- [9] O. Simeone and U. Spagnolini, "Distributed time synchronization in wireless sensor networks with coupled discrete-time oscillators," *EURASIP J. on Wireless Communications and Networking*, pp. 1–13, 2007.
- [10] I. Councill, L. Giles, and P. Teregowda, "Consensus propagation," *IEEE Transactions on Information Theory*, vol. 52, no. 11, pp. 4753–4766, Nov 2006.
- [11] K. Avrachenkov, M. E. Chamie, and G. Neglia, "A local average consensus algorithm for wireless sensor networks," in *Proc. of IEEE Conf. on Distributed Computing in Sensor Systems (DCOSS)*, Barcelona, Spain, Jun 2011, pp. 1–6.
- [12] O. Simeone, U. Spagnolini, G. Scutari, and Y. Bar-Ness, "Physical-layer distributed synchronization in wireless networks and applications," *Physical Communication*, vol. 1, no. 1, pp. 67–83, Mar 2008.
- [13] M. Nokleby, W. U. Bajwa, R. Calderbank, and B. Aazhang, "Gossiping in groups: Distributed averaging over the wireless medium," in *Proc. of the 49th Annual Allerton Conf. on Communication, Control, and Computing*, Monticello (IL), USA., Sep 2011, pp. 1242–1249.
- [14] B. Nazer, A. G. Dimakis, and M. Gastpar, "Local interference can accelerate gossip algorithms," *IEEE J. on Selected Topics in Signal Processing*, vol. 5, no. 4, pp. 876–887, Aug 2011.
- [15] M. Goldenbaum, H. Boche, and S. Stańczak, "Nomographic gossiping for f -consensus," in *Proc. of Intl' Symposium on Modeling and Optimization in Mobile, Ad Hoc and Wireless Networks (WiOpt)*, Paderborn, Germany, May 2012, pp. 130–137.
- [16] A. G. Dimakis, A. D. Sarwate, and M. J. Wainwright, "Geographic gossip: Efficient averaging for sensor networks," *IEEE Transactions on Signal Processing*, vol. 56, no. 3, pp. 1205–1216, Mar 2008.
- [17] M. Feinberg and F. M. Horn, "Dynamics of open chemical systems and the algebraic structure of the underlying reaction network," *Chemical Engineering Science*, vol. 29, pp. 775–787, 1974.
- [18] P. Dittrich and P. Speroni di Fenizio, "Chemical organization theory," *Bulletin of Mathematical Biology*, vol. 69, no. 4, pp. 1199–1231, May 2007.
- [19] M. Feinberg, "Complex balancing in general kinetic systems," *Archive for Rational Mechanics and Analysis*, vol. 49, no. 3, pp. 187–194, Dec 1972.
- [20] T. Meyer, "On chemical and self-healing networking protocols," Ph.D. Thesis, University of Basel, Switzerland, Feb 2011.
- [21] T. Meyer and C. Tschudin, "Chemical networking protocols," in *Proc. of the ACM Workshop on Hot Topics in Networks (HotNets)*, Oct 2009.
- [22] A. Varga and R. Hornig, "An overview of the OMNeT++ simulation environment," in *Proc. of SIMUTOOLS*, Marseille, France, 2008, pp. 1–10.
- [23] P. Dittrich, J. Ziegler, and W. Banzhaf, "Artificial chemistries - a review," *Artificial Life*, vol. 7, no. 3, pp. 225–275, Summer 2001.
- [24] H. I. Abrash, "Studies concerning affinity," *J. of Chemical Education*, vol. 63, no. 12, pp. 1044–1047, Dec 1986.
- [25] M. A. Gibson and J. Bruck, "Efficient exact stochastic simulation of chemical systems with many species and many channels," *J. Phys. Chem. A*, vol. 104, no. 9, pp. 1876–1889, Feb 2000.
- [26] D. A. McQuarrie, "Stochastic approach to chemical kinetics," *J. of Applied Probability*, vol. 4, no. 3, pp. 413–478, Dec 1967.
- [27] T. Jahnke and W. Huisinga, "Solving the chemical master equation for monomolecular reaction systems analytically," *J. of Mathematical Biology*, vol. 54, no. 1, pp. 1–26, Sep 2007.
- [28] D. T. Gillespie, "The chemical Langevin equation," *J. Chem. Phys.*, vol. 113, no. 1, Jul 2000.
- [29] R. Olfati-Saber and R. M. Murray, "Consensus problems in networks of agents with switching topology and time-delays," *IEEE Transactions on Automatic Control*, vol. 49, no. 9, pp. 1520–1533, Sep 2004.
- [30] W. Shaochuan and M. G. Rabbat, "Broadcast gossip algorithms for consensus on strongly connected digraphs," *IEEE Transactions on Signal Processing*, vol. 61, no. 16, pp. 3959–3971, Aug 2013.
- [31] G. Shinar, U. Alon, , and M. Feinberg, "Sensitivity and robustness in chemical reaction networks," *SIAM J. Appl. Math.*, vol. 69, no. 4, pp. 977 – 998, 2009.
- [32] R. Carli, F. Fagnani, P. Frasca, and S. Zampieri, "Gossip consensus algorithms via quantized communication," *Automatica*, vol. 46, no. 1, pp. 70–80, 2010.
- [33] F. Horn and R. Jackson, "General mass action kinetics," *Archive for Rational Mechanics and Analysis*, vol. 47, no. 2, pp. 81–116, 1972.
- [34] P. D. Leenheer and D. Angeli, "Monotonicity and convergence in chemical networks," in *Proc. of IEEE Conf. on Decision and Control, and European Control Conf. (CDC-ECC)*, Seville, Spain, Dec 2005, pp. 2362–2367.